Acta Astronautica 125 (2016) 174–182

Contents lists available at ScienceDirect

Acta Astronautica

journal homepage: www.elsevier.com/locate/actaastro

Invited Paper

Attitude reconstruction of ROSETTA's Lander PHILAE using two-point magnetic field observations by ROMAP and RPC-MAG

Philip Heinisch [a,*], Hans-Ulrich Auster [a], Ingo Richter [a], David Hercik [a], Eric Jurado [b], Romain Garmier [c], Carsten Güttler [d], Karl-Heinz Glassmeier [a,d]

[a] Institut für Geophysik und extraterrestrische Physik, Technische Universität Braunschweig, Mendelssohnstrasse 3, D-38106 Braunschweig, Germany
[b] Centre National d'Études Spatiales ,18 Avenue Édouard Belin, 31400 Toulouse, France
[c] CS-SI, Parc de la Plaine, 5 Rue Brindejonc des Moulinais, 31506 Toulouse, France
[d] Max-Planck-Institut für Sonnensystemforschung, Justus-von-Liebig-Weg 3, D-37077 Göttingen, Germany

ARTICLE INFO

Article history:
Received 14 August 2015
Received in revised form
15 November 2015
Accepted 2 December 2015
Available online 12 December 2015

Keywords:
PHILAE
ROSETTA
ROMAP
RPC-MAG
Attitude

ABSTRACT

As part of the European Space Agency's ROSETTA Mission the Lander PHILAE touched down on comet 67P/Churyumov–Gerasimenko on November 12, 2014. The magnetic field has been measured onboard the orbiter and the lander. The orbiter's tri-axial fluxgate magnetometer RPC-MAG is one of five sensors of the ROSETTA Plasma Consortium. The lander is also equipped with a tri-axial fluxgate magnetometer as part of the ROSETTA Lander Magnetometer and Plasma-Monitor package (ROMAP). This unique setup makes a two point measurement between the two spacecrafts in a relatively small distance of less than 50 km possible. Both magnetometers were switched on during the entire descent, the initial touchdown, the bouncing between the touchdowns and after the final touchdown. We describe a method for attitude determination by correlating magnetic low-frequency waves, which was tested under different conditions and finally used to reconstruct PHILAE's attitude during descent and after landing. In these cases the attitude could be determined with an accuracy of better than $\pm 5^{\circ}$. These results were essential not only for PHILAE operations planning but also for the analysis of the obtained scientific data, because nominal sources for this information, like solar panel currents and camera pictures could not provide sufficient information due to the unexpected landing position.

1. Introduction

The release of the Lander PHILAE [1] to the cometary surface was one of the major scientific and technical achievements of the ROSETTA Mission [2]. Onboard of both, orbiter [3] and lander [4], fluxgate magnetometers measured the ambient magnetic field for investigating the plasma environment and magnetization of comet 67P/Churyumov–Gerasimenko (67P). Because PHILAE is not equipped with dedicated navigation instruments, its position and attitude during the Descent and Landing Phase (SDL) and First Science Sequence (FSS) must be reconstructed using results from the scientific instruments. Nominally this should have been done using CIVA [5] panoramic images and an analysis of the

* Corresponding author. Tel.: +49 (0) 531 391 5230.
E-mail address: p.heinisch@tu-bs.de (P. Heinisch).

http://dx.doi.org/10.1016/j.actaastro.2015.12.002

different solar panel currents [6] together with CONSERT [7] ranging results. Unfortunately, the conditions for attitude determination during both, SDL and FSS were more complex than anticipated. Due to a malfunction of its harpoons, PHILAE bounced three times after the first touchdown before coming to a final rest [8,9]. At the final landing site, illumination conditions were worse than expected for the nominal landing site, as only for about two hours of day light per cometary day three out of six solar panels were illuminated and generated power [10]. Hence insufficient information for attitude reconstruction, based solely on solar panel currents, was available [6]. As CIVA images [9] clearly indicate, PHILAE was tilted towards the comet surface after the final touchdown and some of the cameras were pointing away from the comet. It was therefore not possible to identify landmarks on any of the CIVA images, that could reliably be used for attitude reconstruction. Based on PHILAE's self shadow it was only possible to estimate the solar position above the comet for the specific time the images were taken, which was not sufficient for complete attitude determination. [6] The tri-axial fluxgate magnetometer of the ROSETTA Lander Magnetometer and Plasma Monitor package (ROMAP) [4] as well as the two tri-axial fluxgate magnetometers from the ROSETTA Plasma Consortium (RPC-MAG) [2] were switched on during SDL and the first part of the FSS, which gave the unique opportunity to use the combined results from both experiments to reconstruct the attitude by magnetic field measurements. This method was initially only intended as a possible backup approach to the above-mentioned options. Actually, the presence of band-limited low-frequency magnetic field oscillations [11] strongly enhanced the possibility to use combined measurements to determine PHILAE's attitude successfully. In contrast to the unfavorable conditions for the two primary methods, conditions for attitude determination by magnetic field comparison were thus much better than anticipated. Therefore, the former backup option, using the comparison of magnetic field variations onboard the orbiter and lander became the primary method for attitude determination. The details of this method and its results are described below.

2. Attitude reconstruction: the method

Attitude reconstruction as presented here is based on correlating magnetic field vector measurements made at the same time at two different points in space, assuming the magnetic field conditions are nearly identical at both locations. If the attitude of the magnetic field sensor at point P is known, but unknown at position Q, then the unknown attitude at point Q can be determined by rotating the sensor coordinate system at Q in such a way that the correlation coefficient between time series of the magnetic field components at Q maximizes with that one at P. Let $\underline{B}_P$ and $\underline{B}'_Q$ be the measured vectors at P and Q respectively and $\underline{B}_Q$ the field vector at location Q after rotation, that is

$$\underline{B}_Q = \underline{\underline{M}} \cdot \underline{B}'_Q \tag{1}$$

with the matrix

$$\underline{\underline{M}} = \begin{pmatrix} 1 & 0 & 0 \\ 0 & \cos(\alpha) & -\sin(\alpha) \\ 0 & \sin(\alpha) & \cos(\alpha) \end{pmatrix} \begin{pmatrix} \cos(\beta) & 0 & \sin(\beta) \\ 0 & 1 & 0 \\ -\sin(\beta) & 0 & \cos(\beta) \end{pmatrix} \begin{pmatrix} \cos(\gamma) & -\sin(\gamma) & 0 \\ \sin(\gamma) & \cos(\gamma) & 0 \\ 0 & 0 & 1 \end{pmatrix} \tag{2}$$

denoting the rotation matrix constructed from the Euler angles α, β, and γ. To reconstruct the attitude of the magnetometer at Q relative to the attitude of the reference magnetometer at P, $\underline{\underline{M}}$ has to be determined in such a way that the correlation coefficient between all components, defined as

$$\overline{\rho} = \frac{1}{3}\left(\frac{\mathrm{Cov}(\underline{B}_{X,Q},\underline{B}_{X,P})}{\sigma(\underline{B}_{X,Q})\sigma(\underline{B}_{X,P})} + \frac{\mathrm{Cov}(\underline{B}_{Y,Q},\underline{B}_{Y,P})}{\sigma(\underline{B}_{Y,Q})\sigma(\underline{B}_{Y,P})} + \frac{\mathrm{Cov}(\underline{B}_{Z,Q},\underline{B}_{Z,P})}{\sigma(\underline{B}_{Z,Q})\sigma(\underline{B}_{Z,P})}\right) \tag{3}$$

where $\mathrm{Cov}(X)$ denotes the covariance of X and $\sigma(X)$ the standard deviation of X, is maximized. This can either be done by solving the extremum problem analytically or by discretizing the angles and for instance using an exhaustive brute force approach to find the angles corresponding to the maximum correlation. Among the two methods described above, the latter was chosen, as it gives the correlation coefficient for each individual angle and allows a detailed analysis of the sensitivity of the tool relative to changes in the individual Euler angles.

As this approach is based on correlating variations in the magnetic field, a prerequisite for this method is a sufficient signal to noise ratio, so that field fluctuations can clearly be separated from the background field and any external interference for example caused by spacecraft (s/c) operations and the noise floor of the instruments which is typically around 10 $\mathrm{pT}/\sqrt{\mathrm{Hz}}$. In addition the field variations have to be clearly detectable at both locations simultaneously. Thus our method is only applicable if a clear fluctuating signal is present. This implies either a sufficiently strong background magnetic field such as a planetary magnetic field or predominating magnetic field fluctuations. When this method is applied to observations in the interplanetary medium, the interplanetary background magnetic field, close to 67P at 3 AU is not sufficiently strong [12] to apply the suggested attitude reconstruction tool, as solar wind fluctuations are smaller than approximately 2 nT [11]. Fortunately upon arrival of the ROSETTA spacecraft in August 2014 at 67P, low frequency waves in the range of 30–50 mHz with amplitudes of $\sim$ 5 nT caused by the solar wind – comet interaction dominated the magnetic-field measurements of the RPC-MAG [11] and ROMAP instruments. An example of these oscillations observed on October 17, 2014 is presented in Fig. 1. This clear signal provides for a most suitable situation to apply our method to RPC-MAG and ROMAP data.

As the set of available observations was much larger than initially anticipated and necessary for attitude reconstruction, it was only possible to select the most suitable intervals. This was done based on whether the fluctuations described above were clearly detectable in the individual intervals. To accomplish this, the magnitude

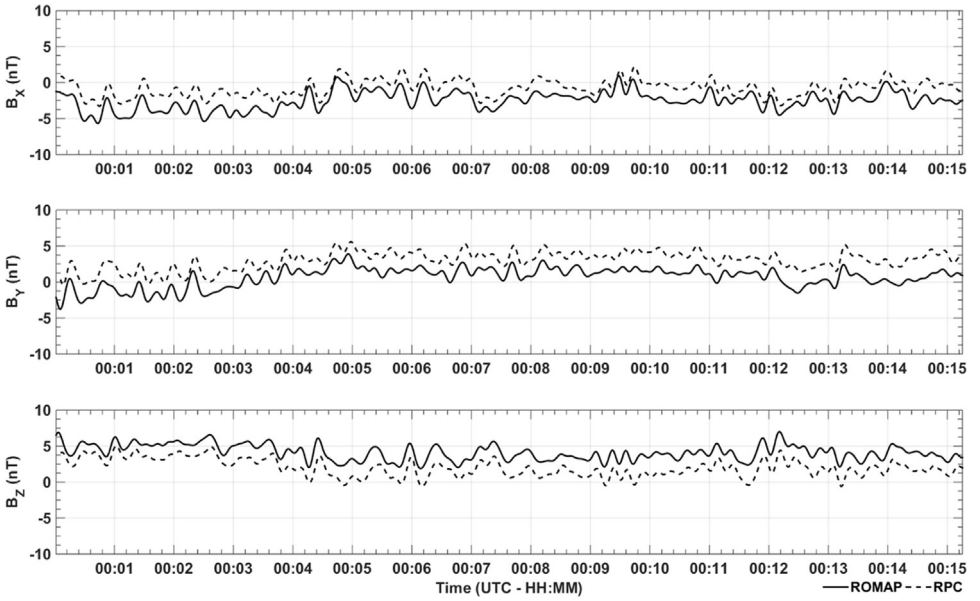

Fig. 1. Low-pass filtered three component magnetic field signal in ROSETTA spacecraft coordinate system observed around midnight on October 17, 2014 by ROMAP (solid line) and RPC-MAG (dashed line) showing 30–50 mHz oscillations.

squared coherence between both concurrent signals defined as

$$C_{P,Q}(f) = \frac{|G_{P,Q}(f)|^2}{G_{P,P}(f) \cdot G_{Q,Q}(f)} \tag{4}$$

where $G(f)$ is the cross-spectral density was calculated for the aforementioned frequency bands. Additional data conditioning was performed prior to the actual attitude determination steps to remove any DC components, offsets and frequency bands affected by local s/c disturbances. The complete data handling is illustrated in the flowchart in Fig. 2.

3. Attitude Reconstruction: THEMIS Tests

To test this method under more realistic space conditions, magnetic field measurements obtained in the solar wind as part of the multi-satellite THEMIS mission [13,14] was used as input. As the attitude of the five satellites is known precisely and the relative distances between the individual satellites varies, these measurements are ideally suited for such tests and the THEMIS magnetometer data provided a valuable verification possibility for the methodology.

A data interval from June 28, 2007 was selected because of clearly visible oscillations of the solar wind magnetic field in the range of $\sim$ 5nT. This is exemplarily displayed in Fig. 3 for the B_Z-components of all five THEMIS spacecraft. The attitude reconstruction results are presented in Table 1. The method shows an overall error for all reconstructed Euler angles of below 3° for all studied cases with the correlation coefficient being above 0.94. In general, the method gives better results with smaller distances between the two selected magnetometers and for datasets with prominent magnetic features.

4. Attitude Reconstruction: First ROSETTA Tests

ROSETTA and PHILAE magnetometer observations made during the post hibernation commissioning, approach and mapping phases [2] were used as input for additional testing. As PHILAE was still attached to ROSETTA the precise attitude was known and could be used as reference to determine the absolute accuracy. After wake-up from deep-space hibernation in January 2014 ROSETTA was in the solar wind at 3.5 AU. Due to low solar wind activity at this heliocentric distance, few global field variations were observed and most of the measurements were unsuitable for attitude reconstruction, because most external field fluctuations were indiscernible from interferences created by ROSETTA and PHILAE. Nevertheless these observations made it possible to gain knowledge about the different s/c interference sources, which were clearly distinguishable from the low background field. Because the boom the ROMAP sensor was mounted to, was still in the stowed position up against the balcony of PHILAE and adjacent to the ROSETTA orbiter, s/c interference were much more prominent due to the close physical proximity of the sensor to the interference sources. This enabled testing under much harsher conditions then could be expected after separation and boom deployment. When ROSETTA approached the increasingly active comet in summer 2014 the conditions changed drastically. Low-frequency waves, caused by the interaction of the solar wind with the comet were detected [11] in the vicinity of 67P, which turned out to be ideally suited for attitude determination.

The correlation coefficients depending on the elevation angle resulting from the attitude determination algorithm applied to two 15 min input intervals of RPC-MAG and ROMAP observations from two different months are shown in Fig. 4. For comparison the algorithm was also

used with two signals from the ground based magnetic observatory in Niemegk [15] rotated in such a way as to represent PHILAE's attitude before separation, to illustrate the best possible results. As PHILAE was mounted to ROSETTA during the cruise phase, PHILAE's attitude relative to ROSETTA remained fixed. In this configuration, only the elevation of the lander relative to the orbiter was nonzero. Therefore, the correlation coefficient is only displayed as a function of elevation, and the remaining two Euler angles are fixed at zero. While the first dataset is dominated by solar wind observed during the approach phase on July 14, 2014, the second is from the close mapping phase on October 17, 2014 and is dominated by waves caused by the comet's interaction with the solar wind as described earlier. In the first case, the algorithm yields a maximum correlation coefficient of 0.68 for the entire range between 78° and 83° elevation, which shows that the resolution is limited to 5° due to the small field variations. As PHILAE was still mounted to ROSETTA, the expected attitude result is known to be 90°. The second case yielded much more precise results thanks to the stronger field variations caused by the comet interaction with the solar wind. The correlation coefficient reached its maximum at an elevation angle of 92°, with a value of 0.91.

For the real attitude determination after lander separation, the first step was to remove any visible s/c disturbances, which was done manually using the information gained during the previous tests. To reduce the risk of errors introduced due to a moving reference frame, the RPC-MAG results were first rotated from a ROSETTA centered frame ('ROS_SPACECRAFT') to a Comet Fixed Frame ('CFF' or '67P/C-G_CK') using the NASA SPICE system [16] based on the official ESA kernels. The center of the CFF is the center of mass of the comet, the *z*-axis is the positive pole of the rotation axis, the *x*-axis is defined by the intersection point between equator and prime meridian and the *y*-axis completes the right handed system. This made it possible to determine PHILAE's attitude directly in relation to the comet without accounting for its rotation. The resulting three component ROMAP signal

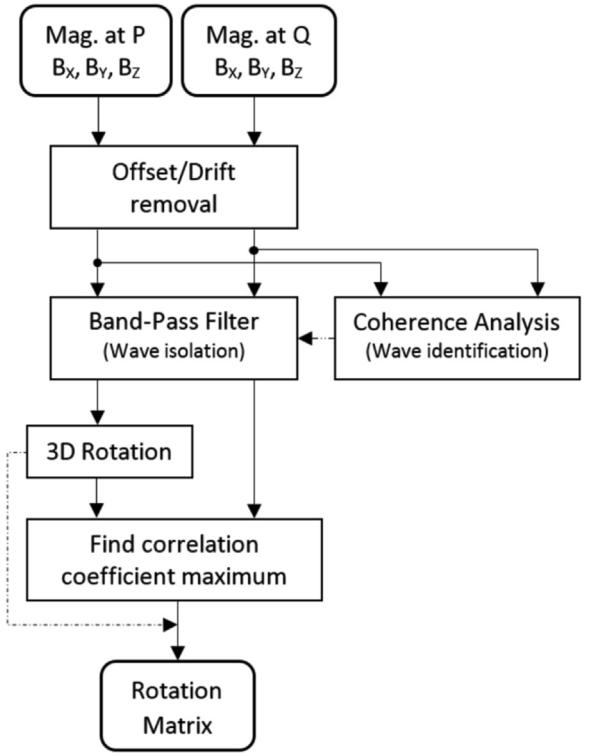

Fig. 2. Flowchart illustrating the individual data processing steps used for the attitude reconstruction tool.

Table 1
Correlation results for the THEMIS test case showing the influence of the propagation delay between different s/c. 'ρ unshifted' was computed without accounting for wave propagation delay. The data was then shifted according to 'Time shift', which was determined by cross correlating the individual datasets and used to calculate 'ρ shifted'. This data was used to reconstruct the s/c attitude and the error relative to the known attitude is given as 'Attitude Error'.

	CE	DE	BE	AD	AB
Distance	59 km	150 km	561 km	2069 km	2980 km
ρ unshifted	0.97	0.96	0.96	0.91	0.92
Time shift	0 s	0 s	0 s	1.3 s	1 s
ρ shifted	0.97	0.96	0.96	0.94	0.95
Attitude Error	0.5°	1°	1°	3°	2°

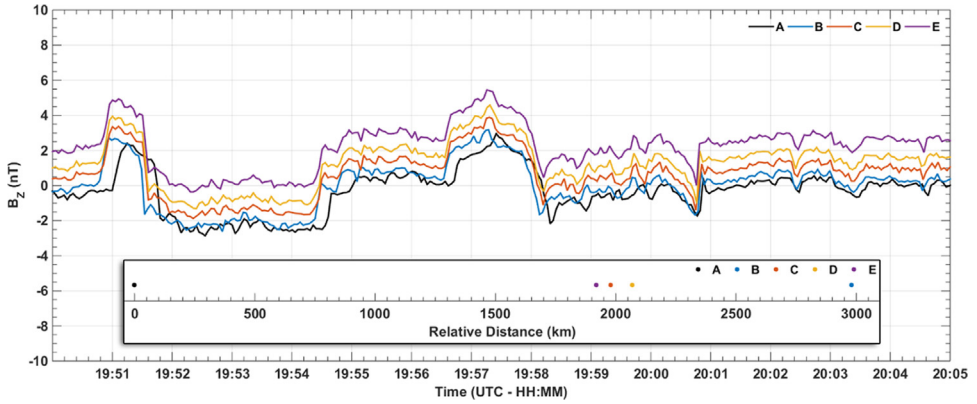

Fig. 3. B_Z-component of a 15 min interval of THEMIS magnetometer solar wind observations from June 28, 2007 and the *s/c* distances relative to THEMIS-A for the same period.

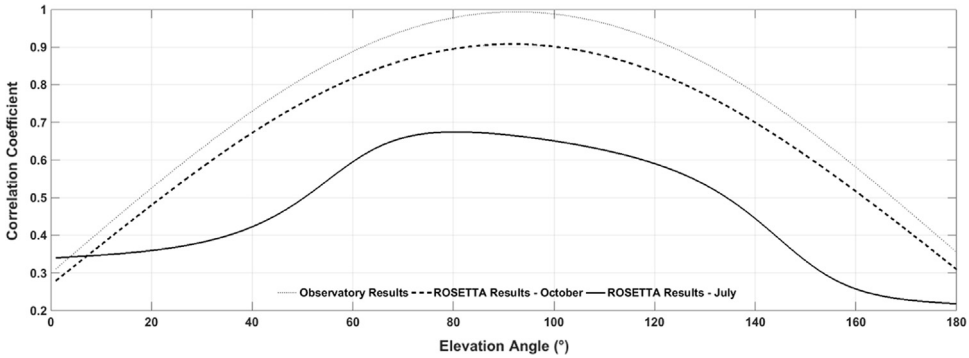

Fig. 4. Correlation coefficients depending on the elevation angle resulting from the attitude determination algorithm based on 15 min observations from July 14, 2014 (solid line) and October 17, 2014 (dashed line). For comparison the method was also used with two signals from the ground based magnetic observatory in Niemegk [15] rotated in such a way as to simulate PHILAE's attitude before separation (dotted line).

was then numerically rotated in order to maximize the correlation between the three magnetic field components of ROMAP and RPC-MAG, as described above. This way a 3D rotation matrix from a PHILAE centered frame ('LDR') to a ROSETTA centered frame was generated. As the orientation of ROSETTA is known, the obtained rotation matrix can be transformed to calculate PHILAE's attitude relative to any reference frame. The available data was separated into individual intervals of approximately 15 min to be able to exclude segments with strong s/c interference or low activity in the magnetic field. This approach also made it possible to do a statistical analysis of the individual results for error estimation. The exact length of the intervals varied, due to packet loss or data corruption during transmission.

5. Attitude reconstruction: descent

To reconstruct the attitude of PHILAE during the SDL phase, the non-translational motion of the lander had to be taken into account. After landing gear and ROMAP boom deployment, it was dominated by a rotation around the *z*-axis with a period increasing from approximately 510–590 s, which was not only reconstructed from ROMAP magnetic field data by using a simple spectral analysis, but also from solar array housekeeping and CONSERT signal strength variations. [6] Using a model of PHILAE's motion, it was possible to reverse most of this rotational movement. Afterwards, the descent dataset was first split into individual intervals of about 15 min. This way, also temporal changes in the rotation frequency could be accounted for by re-fitting the rotation for every interval separately. To de-spin the data, any remaining DC components were first removed from the individual magnetic field components, afterwards the fitted rotation was applied backwards.

The resulting data, now rotated into an artificial inertial reference frame, was then used together with RPC-MAG data as before, to determine the remaining static rotation between lander and orbiter. Together both of these results give the final time-dependent attitude.

Fig. 5 shows an example of the final attitude applied to an interval of ROMAP observations. Before rotation to CFF, the correlation between ROMAP and RPC-MAG was 0.38, after rotation to CFF it increased to 0.74.

6. Attitude reconstruction: landing

The First Science Sequence started automatically after the first touchdown was detected, but PHILAE bounced several times, due to harpoon and cold gas thruster (ADS) malfunctions. After the final touchdown at $17:31:17 \pm 1$ s UTC PHILAE was in a stationary state relative to the comet. Due to the unexpected change in the final landing site and unknown status of PHILAE, previously unscheduled safe blocks without operation of any mechanical parts were inserted, during which ROMAP was switched on. Therefore, ROMAP was operating longer than originally planned. In total about 18.5 h of simultaneous ROMAP and RPC-MAG observations with a sampling rate of 1 Hz are available for attitude determination and scientific interpretation. Additionally about half an hour of measurements from the RPC-MAG inboard (RPC-IB) magnetometer are available at the beginning of the FSS, in addition to the outboard magnetometer (RPC-OB) observations. Afterwards RPC-MAG had to be switched to a different mode due to bandwidth constraints on the orbiter, which lead to the RPC-IB sampling rate becoming unsuitable for this analysis.

One of these input intervals with data from ROMAP and both RPC-OB and RPC-IB is shown in Fig. 6. Even before the ROMAP results were correctly rotated to the CFF, nearly identical magnetic signatures can be identified in the individual components. This is especially obvious in the *z*-component, as by chance the *z*-axis in the CFF and LDR frame were already roughly aligned after the final TD. This confirms that the same low frequency waves can be observed on the surface as well as in orbit around the comet.

A band-pass filter with a lower cutoff-frequency of 5 mHz and an upper cutoff frequency of 60 mHz was used to isolate these low frequency waves. The lower bound was selected to exclude the slow temperature drifts of the instruments due to changes in illumination conditions and to remove any remaining DC offset. Additionally care has to be taken while analyzing these extremely low frequency ranges, as the actual wave amplitudes are most of the time considerably smaller than for waves above 5 mHz. A

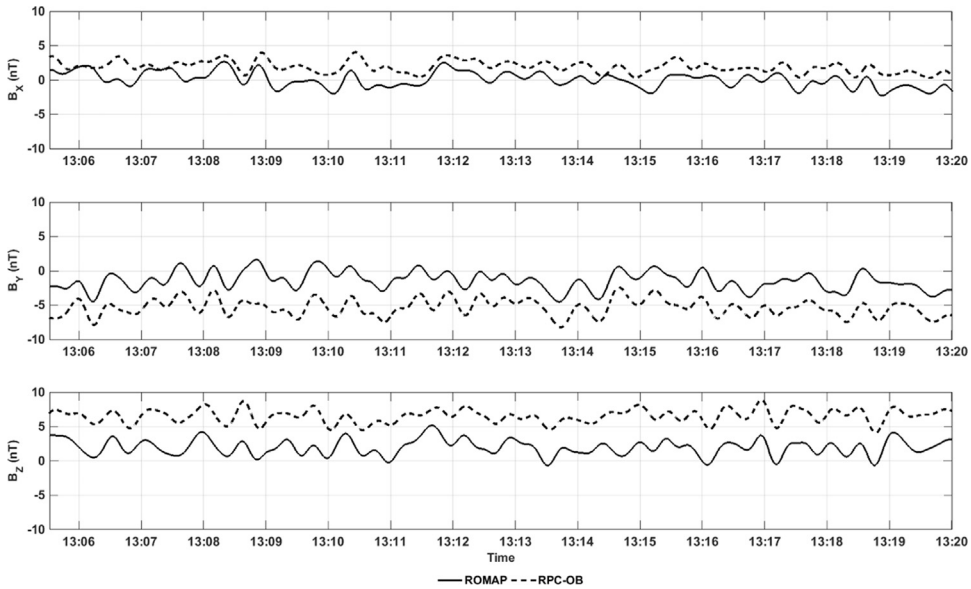

Fig. 5. Interval of processed and filtered ROMAP (solid line) measurements rotated to CFF using the reconstructed SDL attitude and processed and filtered RPC-OB (dashed line) measurements rotated to CFF.

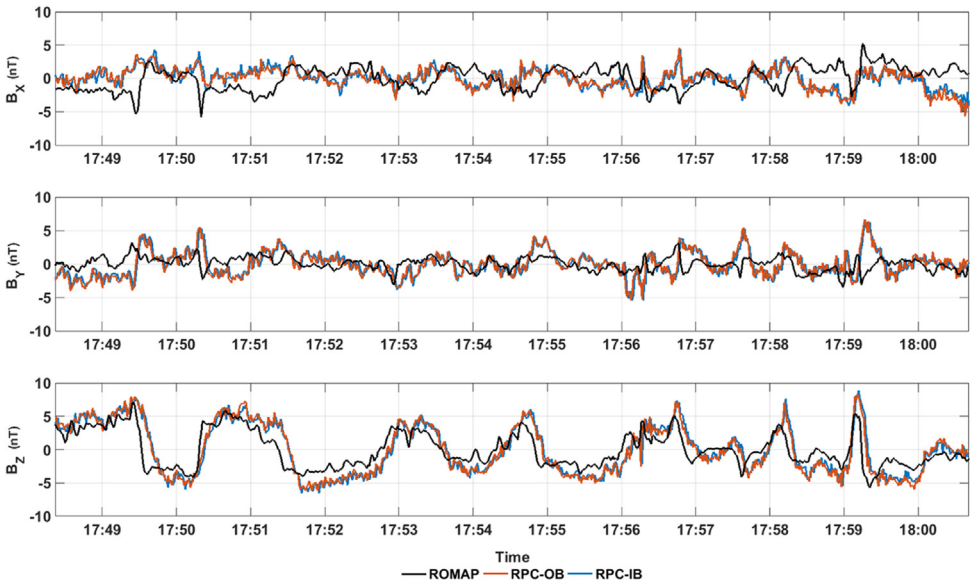

Fig. 6. Interval of calibrated but unfiltered ROMAP (black) measurements in the original LDR frame and calibrated but unfiltered RPC-OB (orange) and RPC-IB (blue) measurements rotated to CFF. (For interpretation of the references to color in this figure caption, the reader is referred to the web version of this paper.)

detailed analysis of the observed low frequency waves showed that they peak around 40 mHz with a Rayleigh-type distribution with most waves being below 75 mHz [11]. To include as many wave events as possible, while still ensuring that no higher frequency s/c interferences negatively impact the results, the upper cutoff frequency was set at 60 mHz. The different frequency characteristics of the possible s/c interference sources, for example by the flywheel or internal heaters could accurately be determined using earlier observations directly after ROSETTA wake-up (see Section 4). As an example that most of the activity falls within this window, the coherence spectrum of the magnitude of ROMAP and RPC-OB for the interval shown in Fig. 6 is presented in Fig. 7.

The results for the three reconstructed Euler angles for the rotation from LDR to CFF for the individual intervals are shown in Fig. 8. To suppress erroneous results from intervals with local field anomalies or s/c disturbances, only intervals with a correlation between both signals of better than $\rho = 0.75$ were considered. The mean rotation angles as indicated in the figure are $\overline{\alpha} = 185^{\circ}$, $\overline{\beta}_Y = 149^{\circ}$ and $\overline{\gamma}_Z = 276^{\circ}$ with corresponding standard deviations of

$\overline{\sigma}_X = 5.26^\circ$, $\overline{\sigma}_Y = 11.46^\circ$ and $\overline{\sigma}_Z = 9.6^\circ$. Based on the highest standard deviation ($\overline{\sigma}_Y$) and using a two σ confidence interval, the overall attitude error is expected to be below $\pm 5^\circ$. These Euler angles translate into the following rotation matrix from the LDR frame to the CFF:

$$\underline{\underline{M}}_{LDR,CFF} = \begin{pmatrix} -0.03994 & 0.98867 & -0.14469 \\ -0.82587 & -0.11417 & -0.55217 \\ -0.56243 & 0.09743 & 0.82107 \end{pmatrix} \quad (5)$$

Fig. 9 shows the same interval as above in Fig. 6 but with the ROMAP results rotated to CFF, using the given matrix. Matching signatures in both signals are obvious. The phase discrepancies between certain signatures, especially visible in the *x*- and *y*-component are most likely not due to an error in the reconstructed attitude or the measurement itself (for example caused by an error in time synchronisation between PHILAE and ROSETTA), but are probably caused by differences in the spatial origin of the individual magnetic waves. The exact mechanism behind this shift is still subject of ongoing research. The reconstructed attitude was checked against the results from an analysis of the sun direction in the panoramic image made by the Comet Infrared and Visible Analyzer (CIVA-P). Even though a direct attitude reconstruction was not possible from these images, the reconstructed sun direction is consistent with the attitude given above within the margins of error. It is also consistent with the solar array illumination, even though some uncertainties remain due to partial shading of cells. [6]

A visualization of PHILAE magnified $25\times$ with the reconstructed attitude on the surface of the comet at the official final landing site known as 'K' or 'ABYDOS' is shown in Fig. 10.

7. Summary

In this paper, we presented a method for reconstructing the attitude of a magnetometer by comparing magnetic field fluctuations with observations from a second magnetometer with known attitude. The algorithm was tested using ground based magnetic observatory, THEMIS and ROSETTA observations. Using this method the attitude of ROSETTA's PHILAE lander on the surface of comet 67P/Churyumov–Gerasimenko as well as during descent has been reconstructed

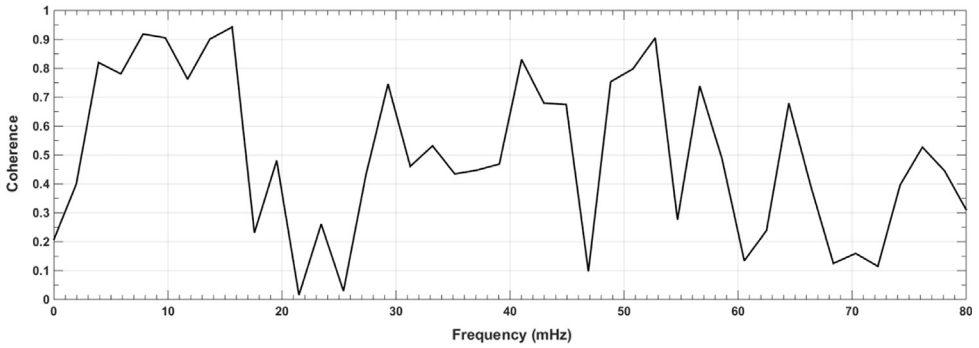

Fig. 7. Coherence spectrum between the magnitude of ROMAP in LDR frame and RPC-OB in CFF for the same 15 min interval as in Fig. 6.

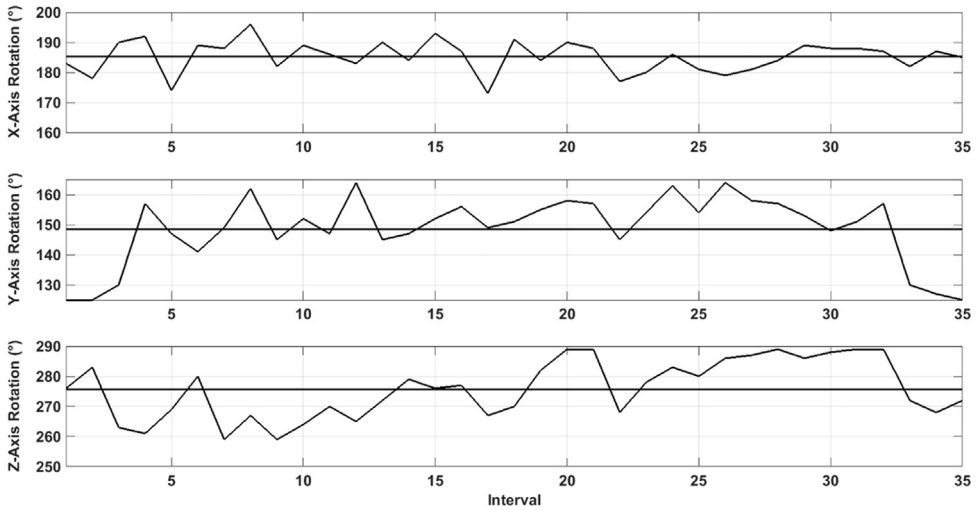

Fig. 8. Euler angles for the rotation from LDR to CFF reconstructed from individual 15 min intervals observed after the final TD, only results yielding a correlation greater than $\rho = 0.75$ are shown.

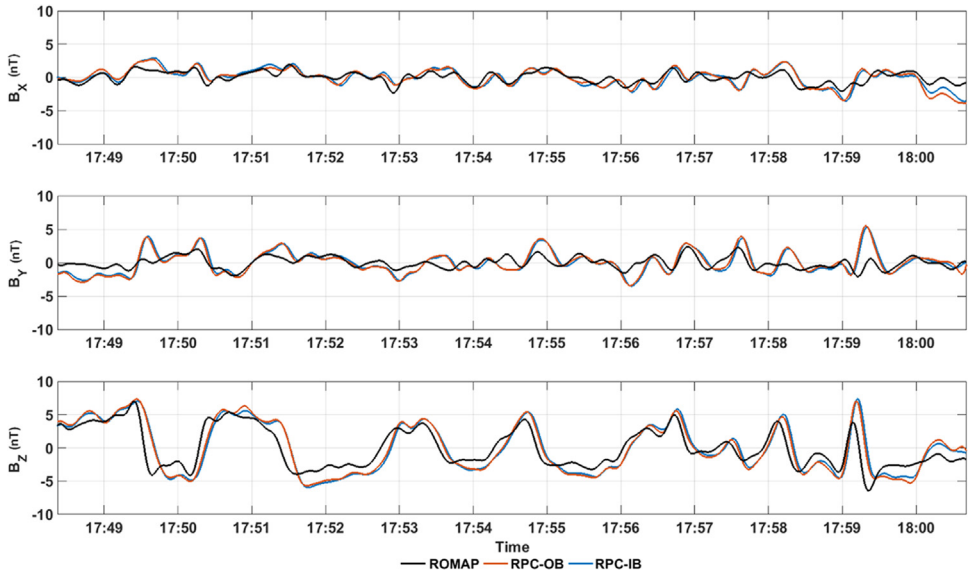

Fig. 9. 15 min interval of processed and filtered ROMAP (black) measurements rotated to CFF using the reconstructed final attitude and processed and filtered RPC-OB (orange) and RPC-IB (blue) measurements rotated to CFF. (For interpretation of the references to color in this figure caption, the reader is referred to the web version of this paper.)

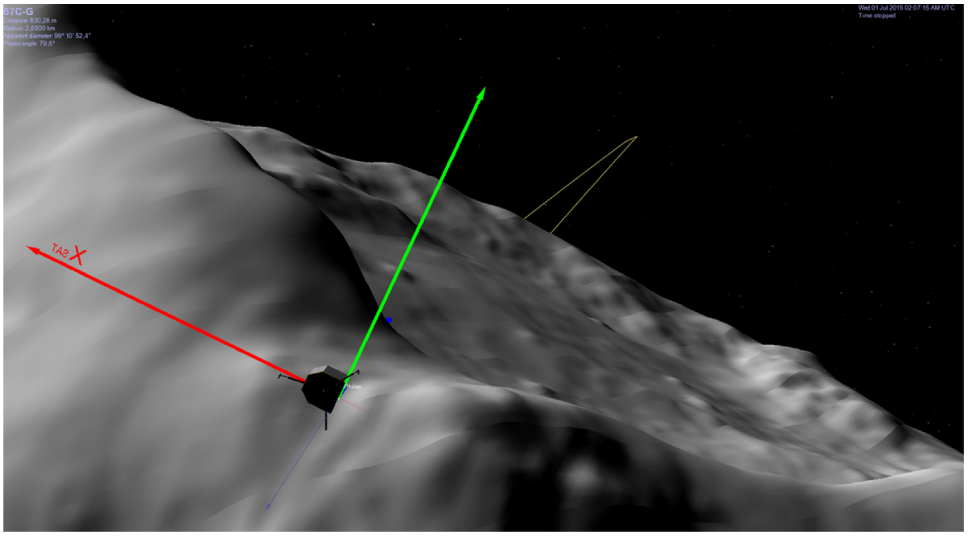

Fig. 10. Visualization of PHILAE (magnified 25 ×) on the comet surface at the official final landing site using the reconstructed attitude. The yellow arc shows part of the ROSETTA orbiter trajectory. (For interpretation of the references to color in this figure caption, the reader is referred to the web version of this paper.)

with accuracies better than $\pm 5^{\circ}$. These results were not only used to confine the possible landing sites, but also as input for the ongoing operational planning.

Acknowledgments

ROSETTA is an ESA mission with contributions from its member states and NASA. The contribution of the ROMAP and RPC-MAG team was financially supported by the German Ministerium für Wirtschaft und Energie and the Deutsches Zentrum für Luft- und Raumfahrt under contract 50QP1401. We are indebted to the whole ROSETTA Mission Team, LCC, SONC, SGS, RMOC for their outstanding efforts making this mission possible. The RPC-MAG and ROMAP magnetometers have been calibrated at the magnetic calibration facility MAGNETSRODE, operated by the Institut für Geophysik und extraterrestrische Physik, TU-Braunschweig. The ROMAP and RPC-MAG data as well as the final attitude products will be made available through the PSA archive of ESA and the PDS archive of NASA. The SPICE kernels used for this work are available as ROS-E/M/A/C-SPICE-6-V1.0 through PSA and PDS.

Appendix A. Supplementary data

Supplementary data associated with this paper can be found in the online version at http://dx.doi.org/10.1016/j.actaastro.2015.12.002.

References

[1] J.-P. Bibring, H. Rosenbauer, H. Boehnhardt, S. Ulamec, J. Biele, S. Espinasse, B. Feuerbacher, P. Gaudon, P. Hemmerich, P. Kletzkine, D. Moura, R. Mugnuolo, G. Nietner, B. Pätz, R. Roll, H. Scheuerle, K. Szegö, K. Wittmann, The ROSETTA Lander PHILAE investigations, Space Sci. Rev. 128 (1–4) (2007) 205–220, http://dx.doi.org/10.1007/s11214-006-9138-2.

[2] K.-H. Glassmeier, H. Boehnhardt, D. Koschny, E. Kührt, I. Richter, The ROSETTA mission: flying towards the origin of the solar system, Space Sci. Rev. 128 (1–4) (2007) 1–21, http://dx.doi.org/10.1007/s11214-006-9140-8.

[3] K.-H. Glassmeier, I. Richter, A. Diedrich, G. Musmann, U. Auster, U. Motschmann, A. Balogh, C. Carr, E. Cupido, A. Coates, M. Rother, K. Schwingenschuh, K. Szegö, B. Tsurutani, Rpc-mag the fluxgate magnetometer in the ROSETTA plasma consortium, Space Sci. Rev. 128 (1–4) (2007) 649–670, http://dx.doi.org/10.1007/s11214-006-9114-x.

[4] H. Auster, I. Apathy, G. Berghofer, A. Remizov, R. Roll, K. Fornacon, K. Glassmeier, G. Haerendel, I. Hejja, E. Kührt, W. Magnes, D. Moehlmann, U. Motschmann, I. Richter, H. Rosenbauer, C. Russell, J. Rustenbach, K. Sauer, K. Schwingenschuh, I. Szemerey, R. Waesch, Romap: ROSETTA magnetometer and plasma monitor, Space Sci. Rev. 128 (1-4) (2007) 221–240, http://dx.doi.org/10.1007/s11214-006-9033-x.

[5] J.-P. Bibring, P. Lamy, Y. Langevin, A. Soufflot, M. Berthé, J. Borg, F. Poulet, S. Mottola, Civa, Space Sci. Rev. 128 (1–4) (2007) 397–412, http://dx.doi.org/10.1007/s11214-006-9135-5.

[6] E. Jurado, T. Martin, E. Canalias, A. Blazquez, R. Garmier, T. Ceolin, P. Gaudon, C. Delmas, J. Biele, S. Ulamec, E. Remetean, A. Torres, J. Laurent-Varin, B. Dolives, A. Herique, Y. Roger, W. Kofman, L. Jorda, V. Zakharov, J.-F. Crifo, A. Rodionov, P. Heinisch, J.-B. Vincent, ROSETTA Lander PHILAE: flight dynamics analyses for landing site selection and post- landing operations, Acta Astronaut. 125 (2016) 65–79.

[7] W. Kofman, A. Herique, J.-P. Goutail, T. Hagfors, I. Williams, E. Nielsen, J.-P. Barriot, Y. Barbin, C. Elachi, P. Edenhofer, A.-C. Levasseur-Regourd, D. Plettemeier, G. Picardi, R. Seu, V. Svedhem, The comet nucleus sounding experiment by radiowave transmission (consert): a short description of the instrument and of the commissioning stages, Space Sci. Rev. 128 (1–4) (2007) 413–432, http://dx.doi.org/10.1007/s11214-006-9034-9.

[8] H.-U. Auster, I. Apathy, G. Berghofer, K.-H. Fornacon, A. Remizov, C. Carr, C. Güttler, G. Haerendel, P. Heinisch, D. Hercik, M. Hilchenbach, E. Kührt, W. Magnes, U. Motschmann, I. Richter, C. T. Russell, A. Przyklenk, K. Schwingenschuh, H. Sierks, K.-H. Glassmeier, The nonmagnetic nucleus of comet 67p/Churyumov–Gerasimenko, Science 349 (6247) (2015), arxiv.org/abs/http://www.sciencemag.org/content/early/2015/04/13/science.aaa5102.full.pdf http://dx.doi.org/10.1126/science.aaa5102, ⟨http://www.sciencemag.org/content/early/2015/04/13/science.aaa5102.abstract⟩.

[9] J.-P. Bibring, Y. Langevin, J. Carter, P. Eng, B. Gondet, L. Jorda, S.L. Mouelic, S. Mottola, C. Pilorget, F. Poulet, M. Vincendon, 67p/Churyumov–Gerasimenko surface properties, as derived from the CIVA panoramic images, Science 349 (6247) (2015), http://dx.doi.org/10.1126/science.aab0671, http://www.sciencemag.org/content/349/6247/aab0671.full.pdf.

[10] J. Biele, S. Ulamec, M. Maibaum, R. Roll, L. Witte, E. Jurado, P. Muñoz, W. Arnold, H.-U. Auster, C. Casas, C. Faber, C. Fantinati, F. Finke, H.-H. Fischer, K. Geurts, C. Güttler, P. Heinisch, A. Herique, S. Hviid, G. Kargl, M. Knapmeyer, J. Knollenberg, W. Kofman, N. Kömle, E. Kührt, V. Lommatsch, S. Mottola, R. Pardo de Santayana, E. Remetean, F. Scholten, K.J. Seidensticker, H. Sierks, T. Spohn, The landing(s) of PHILAE and inferences about comet surface mechanical properties, Science 349 (6247) (2015), http://dx.doi.org/10.1126/science.aaa9816, arXiv:http://www.sciencemag.org/content/349/6247/aaa9816.full.pdf http://dx.doi.org/10.1126/science.aaa9816, ⟨http://www.sciencemag.org/content/349/6247/aaa9816.abstract⟩.

[11] I. Richter, C. Koenders, H.-U. Auster, D. Frühauff, C. Götz, P. Heinisch, C. Perschke, U. Motschmann, B. Stoll, K. Altwegg, J. Burch, C. Carr ,E. Cupido, A. Eriksson, P. Henri, R. Goldstein, J.-P. Lebreton, P. Mokashi, Z. Nemeth, H. Nilsson, M. Rubin, K. Szegö, B.T. Tsurutani, C. Vallat, M. Volwerk, K.-H. Glassmeier, Observation of a new type of low-frequencywaves at comet 67p/churyumov-gerasimenko, Annales Geophysicae 33 (8) (2015) 1031–1036, http://dx.doi.org/10.5194/angeo-33-1031-2015. URL: http://www.ann-geophys.net/33/1031/2015/.

[12] K. Hansen, T. Bagdonat, U. Motschmann, C. Alexander, M. Combi, T. Cravens, T. Gombosi, Y.-D. Jia, I. Robertson, The plasma environment of comet 67p/Churyumov–Gerasimenko throughout the ROSETTA main mission, Space Sci. Rev. 128 (1–4) (2007) 133–166, http://dx.doi.org/10.1007/s11214-006-9142-6.

[13] V. Angelopoulos, The THEMIS mission, Space Sci. Rev. 141 (1–4) (2008) 5–34, http://dx.doi.org/10.1007/s11214-008-9336-1.

[14] H. Auster, K. Glassmeier, W. Magnes, O. Aydogar, W. Baumjohann, D. Constantinescu, D. Fischer, K. Fornacon, E. Georgescu, P. Harvey, O. Hillenmaier, R. Kroth, M. Ludlam, Y. Narita, R. Nakamura, K. Okrafka, F. Plaschke, I. Richter, H. Schwarzl, B. Stoll, A. Valavanoglou, M. Wiedemann, The THEMIS fluxgate magnetometer, in: J. Burch, V. Angelopoulos (Eds.), The THEMIS Mission, Springer, New York, 2009, pp. 235–264, http://dx.doi.org/10.1007/978-0-387-89820-9_11.

[15] P. Heinisch, H.-U. Auster, Determination of variometer alignment by using variation comparison with di3-flux, J. Indian Geophys. Union 19 (4) (2015) 433–446.

[16] C.H. Acton, Ancillary data services of NASA's navigation and ancillary information facility, Planet. Space Sci. 44 (1) (1996) 65–70, http://dx.doi.org/10.1016/0032-0633(95)00107-7. Planetary data system, ⟨http://www.sciencedirect.com/science/article/pii/0032063395001077⟩.